“Dual layer” self-sorting with Cucurbiturils

Héctor Barbero, Nathan Thompson and Eric Masson*

Department of Chemistry and Biochemistry, Ohio University, Athens, Ohio 45701, United States.

ABSTRACT: Platinum(II) complexes bearing terpyridyl (tpy) and thiolate ligands were used to test the design of a “dual layer” self-sorting system in the presence of Cucurbit[8]uril (CB[8]). Pt(II) thiolates and CB[8] form 2:1 assemblies, with both metallic centers sitting on top of one another at one of the macrocycle portals. We showed that any pair of these CB[8]-secured Pt(II) complex dimers bearing different tpy “heads” and thiolate “tails” scrambles to afford up to 10 ternary assemblies via two processes: (1) supramolecular exchanges (i.e. the egression and ingression of Pt complexes from and into CB[8]), and (2) ligand exchanges between the Pt thiolates. The mixtures of 10 assemblies were fully characterized by nuclear magnetic resonance spectroscopy. While the thiolate tails do not significantly affect the rate of the supramolecular exchanges, they were found to control (1) the kinetics of ligand exchange, with bulkier thiolates causing dramatic rate retardations, as well as (2) the thermodynamics of the self-sorting process, i.e. the distribution of assemblies at equilibrium, via intra-CB[8] assembly interactions between pairs of thiolates. Ligand exchanges are consistently slower than supramolecular exchanges. An associative pathway that involves the formation of dimers of CB[8]-secured Pt dimers (a total of 4 Pt complexes) during the ligand exchange process has been invoked to rationalize the observed kinetics.

INTRODUCTION

Cucurbit[n]urils (CB[n]) are prime building blocks for the design of self-sorting systems, as several members of their family (n = 6 – 8, typically) display high,[1–4] yet contrasted binding affinities with a wide variety of guests in aqueous medium.[1,5–10] We recently showed that Fe(II) and Ir(III) bis-terpyridyl complexes bearing a CB[n]-binding anchor at the 4’-position of the ligand assemble into dynamic oligomers in the presence of CB[8],[11,12] as the latter non-covalently connects two anchors in its cavity. By varying the nature of the 4’-substituent,[11] as well as the charge of additional groups grafted to the tpy ligand,[12] one can control the sequence of the oligomers. (Fe–Ir–)n and (Fe–Ir–Ir–)n (n ~ 10 – 15 at 1.0 mM) are two sequences we have identified so far. We also showed that Pt(II) acetylides flanked by 4’-substituted tpy ligands, instead of arranging into dynamic oligomers in the presence of CB[8], form 2:2 head-to-head and head-to-tail assemblies, as well as unprecedented 2:1 “stacked” complexes, with both Pt tpy units sitting on top of each other at the same CB[8] portal.[13] We showed that dispersive interactions between the tpy units, and possible Pt-Pt interactions, are favored over optimal stabilization of the positively charged complexes by both CB[n] carbonylated rims in a common “unstacked” ternary complex.

In the present study, we wanted to test whether one could design a “dual layer” self-sorting system, i.e. form assemblies that can self-sort or rearrange based on two concomitant processes, and control the rates of both processes to obtain various and well-characterized distributions of assemblies. The 2:1 Pt-based stacked motif is ideal for such a design, as Pt(II) tpy complexes bearing different CB[8]-binding heads (**a** and **b**, for example, see Figure 1) can undergo supramolecular exchanges, and form up to 3 ternary complexes, **a**·**a**·CB[8], **b**·**b**·CB[8] and **a**·**b**·CB[8]. Furthermore, grafting thiolates to the Pt centers affords Pt complexes with various degrees of ligand lability in aqueous medium. A pair of Pt thiolates with

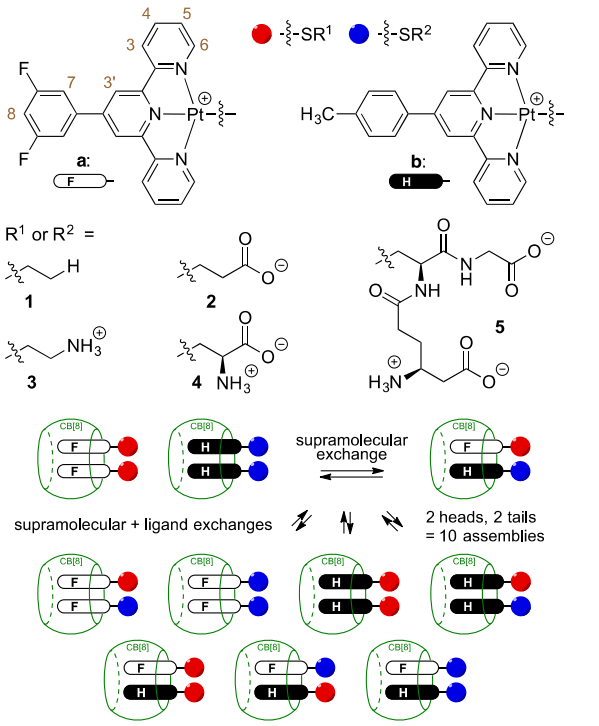

Figure 1. “Dual-layer” self-sorting via supramolecular and ligand exchanges with a pair of CB[8]-secured Pt(II) thiolate dimers.

different CB[8]-binding heads and different thiolate ligands (complexes **1a** and **2b**, for example, see Figure 1), can then undergo self-sorting by ligand exchange towards a set of 4 complexes **1a**, **1b**, **2a** and **2b**. Layering both supramolecular and ligand exchange processes can afford up to 10 complexes: **1a**·**1a**·CB[8], **1a**·**1b**·CB[8], **1a**·**2a**·CB[8], **1a**·**2b**·CB[8], **1b**·**1b**·CB[8], **1b**·**2a**·CB[8], **1b**·**2b**·CB[8], **2a**·**2a**·CB[8], **2a**·**2b**·CB[8] and **2b**·**2b**·CB[8] (see Figure 1). For any number of Pt tpy heads h and thiolate tails t, the maximum number of possible supramolecular assemblies N is the number of multisets of cardinality 2, with elements taken from a finite set of cardinality $h{\cdot}t$ (see equation 1). The maximum number of heteroternary complexes is the number of 2-combinations from a set of $h{\cdot}t$ elements, and the maximum number of homoternary complexes is $h{\cdot}t$.

$$N = \left(\binom{ht}{2}\right) = \binom{ht+1}{2} = \frac{(ht+1)!}{2!(ht-1)!} = \frac{ht(ht+1)}{2} \qquad (1)$$

RESULTS AND DISCUSSION

We prepared tpy ligands **a** and **b** with 3,5-difluorophenyl and tolyl heads, respectively, and their corresponding Pt(II) chloride derivatives using known procedures.[11,13,14] "Stacked" homoternary complexes (PtCl·**a**)$_2$·CB[8] and (PtCl·**b**)$_2$·CB[8] are then readily formed in a phosphate-buffered deuterium oxide solution (50 mM Na^+, pH* 7.5) upon addition of 0.50 equiv. CB[8] (see Figure 2). Very conveniently, the corresponding CB[8]-bound Pt thiolates **1a**$_2$·CB[8] – **5b**$_2$·CB[8] are again obtained in situ by simple addition of the corresponding thiol **1** – **5** (1.0 equivalent) to solutions of complexes (PtCl·**a**)$_2$·CB[8] and (PtCl·**b**)$_2$·CB[8]. A density functional theory-optimized structure of complex **1a**$_2$·CB[8] is presented in Figure 2 (B97-3c functional,[15] def2-mTZVP basis sets,[16] in conjunction with the COSMO solvation model).[17]

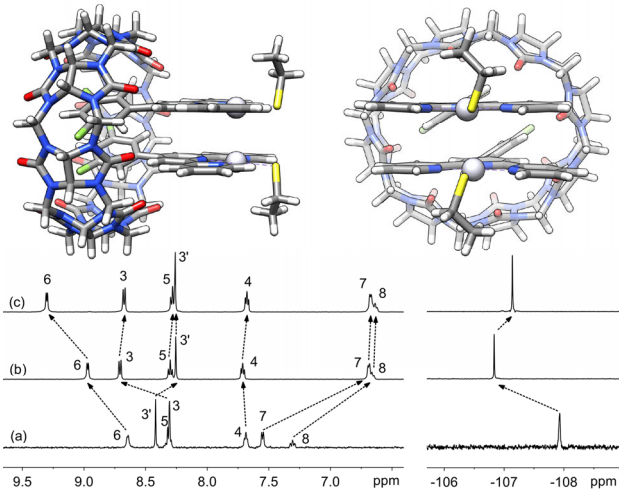

Figure 2. Optimized structure of complex **1a**$_2$·CB[8] (B97-3c/ def2-mTZVP+COSMO). ^{1}H NMR and ^{19}F NMR spectra of (a) complex PtCl·**a**, (b) assembly (PtCl·**a**)$_2$·CB[8], and (c) assembly **1a**$_2$·CB[8]. See Figure 1 for numbering.

^{1}H nuclear magnetic resonance experiments (NMR) showed that ligand exchange is quantitative in less than 10 min. The hydrogen nuclei at positions 6 and 6" (see Figure 2 and Figure 1 for numbering) undergo a downfield shift (approximately 0.5 ppm), while the remaining set of aromatic hydrogens only experience very minor shifts. Given the large separation between the Pt center and the tolyl and 3,5-difluorophenyl tpy heads, their methyl and fluorine ^{1}H and ^{19}F NMR signals are barely shifted upon reaction with thiols **1** – **5** (0.08 and 0.3 ppm on average, respectively). We note that hydrogens at positions 3 – 6, 3" – 6" and 3' become diastereotopic when chiral thiols **4** and **5** are attached to the Pt center, as illustrated by the splitting of the corresponding signals (see NMR spectra in the SI section). Addition of the thiols to the solutions of complexes (PtCl·**a**)$_2$·CB[8] or (PtCl·**b**)$_2$·CB[8] triggered a marked color change from yellow to red, as bathochromic shifts of the ^{1}[dπ(Pt)→π*(terpy)] metal-to-ligand charge transfer band (^{1}MLCT)[18,19] are detected by UV-Vis spectroscopy (see UV-Vis absorption spectra in the SI section). None of the Pt(II) sulfide complexes are emissive. We then combined complexes **1a**$_2$·CB[8] and **2b**$_2$·CB[8] at 25 °C, and monitored the supramolecular and ligand exchanges by ^{1}H and ^{19}F NMR spectroscopy (see Figure 3). A new ^{19}F NMR signal appeared shortly after mixing both complexes (2 h), 0.95 ppm upfield from the one corresponding to complex **1a**$_2$·CB[8]. As the large chemical shift suggested a clear change in environment around the difluoroaryl head,[11–13] we tentatively assigned the new signal to heteroternary complex **1a**·**2b**·CB[8]. Spectra recorded between 2 and 48 h showed that the concentration of the heteroternary complex further increased to the expense of its homo counterparts (see Figure 3, spectra b and c). After 95 h, the number of signals then gradually increased to 8, distributed between two groups of 4. As mentioned earlier, up to 10 assemblies can be obtained, 7 of them containing a fluorinated tpy head (**1a**·**1a**·CB[8], **1a**·**1b**·CB[8], **1a**·**2a**·CB[8], **1a**·**2b**·CB[8], **1b**·**2a**·CB[8], **2a**·**2a**·CB[8] and **2a**·**2b**·CB[8]). In the absence of any overlap, each of these assemblies gives rise to one ^{19}F NMR signal, except heteroternary complex **1a**·**2a**·CB[8] that displays two signals, thereby bringing the total number of signals to 8. Three complexes bear a pair of difluoroaryl heads (**1a**·**1a**·CB[8], **1a**·**2a**·CB[8] and **2a**·**2a**·CB[8]), hence the presence of 4 signals at approximately -107.3 ppm, and 4 complexes bear one tolyl and one difluoroaryl head (**1a**·**1b**·CB[8], **1a**·**2b**·CB[8], **1b**·**2a**·CB[8] and **2a**·**2b**·CB[8]; see the group of 4 signals at -108.2 ppm in Figure 3).

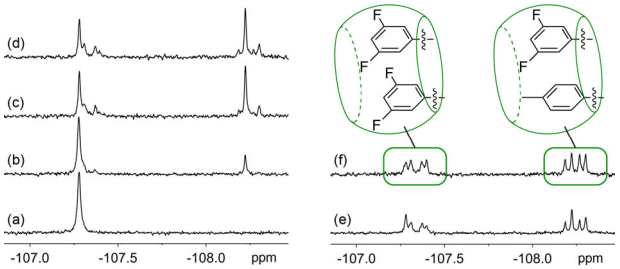

Figure 3. ^{19}F NMR spectra of an equimolar mixture of complexes **1a**$_2$·CB[8] and **2b**$_2$·CB[8] (a) immediately after mixing, and after (b) 7 h, (c) 48 h, (d) 72 h, (e) 95 h and (f) 120 h.

To assign each signal to its corresponding assembly, we designed a series of self-sorting experiments starting from a pair of homoternary assemblies sharing either the same tpy head or thiolate ligand (see Figure 4). The supramolecular exchange of complexes **1a**$_2$·CB[8] and **2a**$_2$·CB[8] readily afforded heteroternary complex **1a**·**2a**·CB[8], and allowed us to assign the group of 4 downfield shifted signals unambiguously (spectra a – c). The exchange between complexes **1a**$_2$·CB[8] and **1b**$_2$·CB[8], as well as between complexes **2a**$_2$·CB[8] and **2b**$_2$·CB[8], allows the unambiguous assignment of the signals pertaining to heteroternary complexes **1a**·**1b**·CB[8] and **2b**·**2b**·CB[8] (spectra d and e). Finally, complexes **1a**$_2$·CB[8] and **2b**$_2$·CB[8] (spectra f and g), as well as complexes **1b**$_2$·CB[8] and **2a**$_2$·CB[8] (spectra h and i) were combined and analyzed after significant scrambling of the tpy heads inside CB[8] but limited ligand exchange (48 h), as well as after complete ligand exchange (200 h). Signals corresponding to assemblies **1a**·**2b**·CB[8] and **1b**·**2a**·CB[8] could then be unambiguously assigned. Combining complexes **1a**$_2$·CB[8] and **2b**$_2$·CB[8] (spectrum g), or **1b**$_2$·CB[8] and **2a**$_2$·CB[8] (spectrum i) returns a very similar mixture of assemblies at 200 h, as supramolecular and ligand exchanges have reached equilibrium.

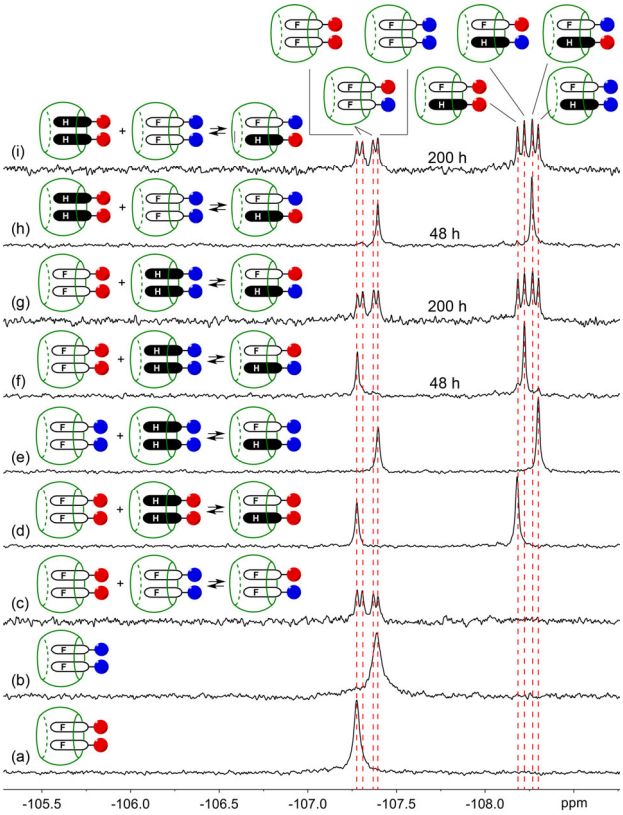

Figure 4. Speciation of CB[8]-secured Pt(II) thiolate dimers. "1/2" coefficients preceeding homoternary complexes are omitted for clarity.

A similar assignment was carried out for assemblies **3b**$_2$·CB[8], **4b**$_2$·CB[8] (in part, due to signal overlaps) and **5b**$_2$·CB[8], respectively, when exchanging with assembly **1a**$_2$·CB[8] (see SI section).

We then tried to separate the supramolecular exchange process (i.e. the scrambling of the tpy heads at the CB[8] portal) from the thiolate ligand exchange, and to assess their respective rates. We started by monitoring at 25 °C the **1a**$_2$·CB[8]/**1b**$_2$·CB[8] and **2a**$_2$·CB[8]/**2b**$_2$·CB[8] pairs of assemblies, as those only afford heteroternary complexes **1a**·**1b**·CB[8] (and **2a**·**2b**·CB[8]) via supramolecular exchanges (see Equilibrium (2) and Figure 5a; k_1 and k_{-1} are rate constants of the forward and reverse reactions, respectively). A plot of the concentration of homoternary complex **1a**$_2$·CB[8] (or **2a**$_2$·CB[8]) as a function of time affords rates k_1 = 1.2 (± 0.1) × 10^{-5} s^{-1} and 6.6 (± 0.5) × 10^{-6} s^{-1}, respectively, using equation (3), as long as the concentrations of both pairs of homoternary complexes at mixing time are equal.

$$\frac{1}{2}\mathbf{1a}_2\cdot\mathrm{CB[8]} + \frac{1}{2}\mathbf{1b}_2\cdot\mathrm{CB[8]} \rightleftarrows \frac{1}{2}\mathbf{1a}\cdot\mathbf{1b}\cdot\mathrm{CB[8]} + \frac{1}{2}\mathbf{1b}\cdot\mathbf{1a}\cdot\mathrm{CB[8]} \qquad (2)$$

$$\frac{[\mathbf{1a}_2\cdot\mathrm{CB[8]}]_t}{[\mathbf{1a}_2\cdot\mathrm{CB[8]}]_0} = 1 - \frac{k_1}{k_1+k_{-1}}(1 - e^{-(k_1+k_{-1})t}) \qquad (3)$$

Separating both supramolecular and ligand exchange processes when they operate concomitantly on a mixture of up to 10 assemblies is extremely challenging. To simplify the treatment, we considered generic equilibrium (4), where ***x*a**$_2$·CB[8] (or ***x*b**$_2$·CB[8]) represents the sum of the concentrations of all homoternary complexes bearing tpy ligand **a** (or ligand **b**, see equations 5 and 6); ***x*a**·***x*b**·CB[8] represents the sum of the concentrations of all heternoternary complexes with a pair of tpy ligands **a** and **b** (equation 7). An apparent, average rate constant can then be obtained with reasonable precision using equation (3), as long as the different thiolates do not cause wide variations in rates of supramolecular exchanges (see Figure 5b).

$$\frac{1}{2}\boldsymbol{x}\mathbf{a}_2\cdot\mathrm{CB[8]} + \frac{1}{2}\boldsymbol{x}\mathbf{b}_2\cdot\mathrm{CB[8]} \rightleftarrows \frac{1}{2}\boldsymbol{x}\mathbf{a}\cdot\boldsymbol{x}\mathbf{b}\cdot\mathrm{CB[8]} + \frac{1}{2}\boldsymbol{x}\mathbf{b}\cdot\boldsymbol{x}\mathbf{a}\cdot\mathrm{CB[8]} \qquad (4)$$

$$[\boldsymbol{x}\mathbf{a}_2\cdot\mathrm{CB[8]}] = [\mathbf{1a}_2\cdot\mathrm{CB[8]}] + [\mathbf{1a}\cdot\mathbf{2a}\cdot\mathrm{CB[8]}] + [\mathbf{2a}_2\cdot\mathrm{CB[8]}] \qquad (5)$$

$$[\boldsymbol{x}\mathbf{b}_2\cdot\mathrm{CB[8]}] = [\mathbf{1b}_2\cdot\mathrm{CB[8]}] + [\mathbf{1b}\cdot\mathbf{2b}\cdot\mathrm{CB[8]}] + [\mathbf{2b}_2\cdot\mathrm{CB[8]}] \qquad (6)$$

$$[\boldsymbol{x}\mathbf{a}\cdot\boldsymbol{x}\mathbf{b}\cdot\mathrm{CB[8]}] = [\mathbf{1a}\cdot\mathbf{1b}\cdot\mathrm{CB[8]}] + [\mathbf{1a}\cdot\mathbf{2b}\cdot\mathrm{CB[8]}] + [\mathbf{1b}\cdot\mathbf{2a}\cdot\mathrm{CB[8]}] + [\mathbf{2a}\cdot\mathbf{2b}\cdot\mathrm{CB[8]}] \qquad (7)$$

The apparent rate of heteroternary complex formation starting from the **1a**$_2$·CB[8]/**2b**$_2$·CB[8] pair is 7.9 (± 0.3) × 10^{-6} s^{-1}, in line with rates obtained for the **1a**$_2$·CB[8]/**1b**$_2$·CB[8] and **2a**$_2$·CB[8]/**2b**$_2$·CB[8] pairs (1.2 × 10^{-5} s^{-1} and 6.6 × 10^{-6} s^{-1}, see above). Rates of supramolecular exchanges starting from pairs **3b**$_2$·CB[8]/**1a**$_2$·CB[8], **4b**$_2$·CB[8]/**1a**$_2$·CB[8] and **5b**$_2$·CB[8]/**1a**$_2$·CB[8] pairs are 1.4 (± 0.1) × 10^{-5}, 7.0 (± 0.2) × 10^{-6} and 7.7 (± 0.1) × 10^{-6} s^{-1}, respectively. Half-lives, calculated using equation 8, and understood as the time needed to consume half of the reactant compared to equilibrium conditions, range from 8 to 16 h at 25 °C. The precise fit and the uniform exchange rates confirm our hypothesis that the thiolate tails do not significantly affect the kinetics of supramolecular exchanges.

$$t_{1/2} = \frac{\ln 2}{k_1 + k_{-1}} \qquad (8)$$

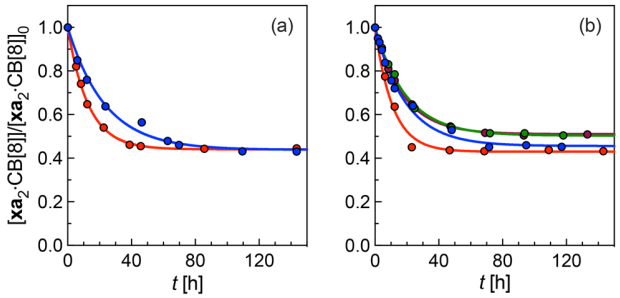

Figure 5. (a) Concentrations of assembly **1a**$_2$·CB[8] (red dots and fit) and **2a**$_2$·CB[8] (blue dots and fit) as a function of time and normalized at t = 0, when allowed to scramble with stoichiometric amounts of assemblies **1b**$_2$·CB[8] and **2b**$_2$·CB[8], respectively. (b) Concentrations of assemblies ***x*a**$_2$·CB[8] (as defined in equations 5 – 7) as a function of time and normalized at t = 0, when assembly **1a**$_2$·CB[8] is allowed to scramble with stoichiometric amounts of assemblies **2b**$_2$·CB[8] (in blue), **3b**$_2$·CB[8] (in red), **4b**$_2$·CB[8] (in green) and **5b**$_2$·CB[8] (in violet; almost overlapped with the **4b**$_2$·CB[8] series).

We then used an approximation similar to equilibrium 4 and equations 5 – 7 to isolate the rates of the ligand exchange process. We considered equilibrium 9 between Pt thiolates **1a** and **2b**, regardless of how they undergo supramolecular self-sorting in the presence of CB[8]. The total concentrations of Pt complex **1a**, for example, is obtained using equation 10 (similar equations can be used to quantify the other 3 complexes in equilibrium 9). A plot of the total concentration of complex **1a** as a function of time (normalized at t = 0) does not show a simple exponential decay (see Figure 6). Carboxylate **2** (blue dots) and ammonium **3** (red dots) exchange slowly with ethylthiolate (**1**) during the first few hours of the process, before accelerating towards the final equilibrium. Approximate half-lives of Pt(II) complexes **2b** and **3b** are 81 and 59 h, respectively, at 25 °C. L-Glutathione (**5**), to the contrary, does not undergo any exchange with ethylthiolate (see green dots in Figure 6). Unfortunately, L-cysteine ligand (**4**) did not allow us to measure the concentration of all required species due to overlaps in the heteroternary region of the ^{19}F NMR spectrum.

$$\frac{1}{2}\mathbf{1a} + \frac{1}{2}\mathbf{2b} \rightleftarrows \frac{1}{2}\mathbf{1b} + \frac{1}{2}\mathbf{2a} \qquad (9)$$

$$[\mathbf{1a}] = [\mathbf{1a}\cdot\mathbf{2b}\cdot\mathrm{CB}[8]] + [\mathbf{1a}\cdot\mathbf{2a}\cdot\mathrm{CB}[8]] + [\mathbf{1a}\cdot\mathbf{1b}\cdot\mathrm{CB}[8]] + 2\cdot[\mathbf{1a}_2\cdot\mathrm{CB}[8]] \qquad (10)$$

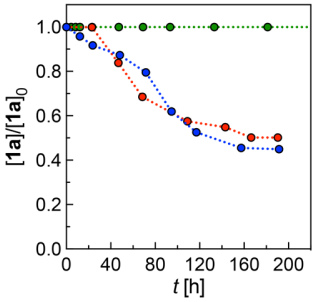

Figure 6. Total concentrations of Pt(II) complex **1a** as a function of time and normalized at t = 0, when CB[8]-secured dimer **1a**$_2$·CB[8] is allowed to scramble with stoichiometric amounts of assemblies **2b**$_2$·CB[8] (blue dot), **3b**$_2$·CB[8] (red dots) and **5b**$_2$·CB[8] (green dots).

The contrasted kinetics of the ligand exchange prompted us to investigate the mechanism of the exchange. In order to isolate it from the supramolecular exchange in the presence of CB[8], we prepared complexes **1a**·CB[7] and **2b**·CB[7] – **5b**·CB[7] in situ, from the corresponding PtCl·**a**·CB[7] and PtCl·**b**·CB[7] precursors. CB[7]-bound Pt complexes were used instead of the free complexes, as those are insoluble in aqueous medium. We then allowed pairs of CB[7]-bound Pt complexes (such as assemblies **1a**·CB[7] and **2b**·CB[7]) to undergo ligand exchange. The only exchange we managed to monitor by NMR spectroscopy with acceptable accuracy (see SI section) was the one between complexes **3b**·CB[7] and **1a**·CB[7], with a half-life of the latter as short as 2 min at 25 °C (rate of conversion 4.0 (± 0.4) × 10^{-3} s^{-1}). All other exchanges proceeded even faster, including L-glutathione ligand (**5**) which did not suffer exchange in CB[8]-secured assemblies. We estimate CB[7]-bound Pt thiolates to undergo ligand exchange at least 1,700 times faster than their corresponding CB[8] assemblies (based on complexes **3b**·CB[7] and **3b**$_2$·CB[8]).

At least three mechanisms can be considered for ligand exchange: (1) a dissociative process, with heterolytic cleavages of the pair of Pt-S bonds, followed by recombination; (2) two associative processes involving substitution of the pair of thiolates with water, followed by recombination; and (3) a single associative process with the formation of a Pt thiolate dimer leading to recombination. Substitution reactions in d^8 square-planar metal complexes are generally of an associative nature,[20,21] and the participation of the solvent is practically negligible in Pt(II) thiolate complexes.[22,23] If the first pathway were valid, treating complex **1a**·CB[7] with free cysteamine (**3**) should exchange much faster than Pt complex **3b**·CB[7] with assembly **1a**·CB[7] (as those Pt complexes are stable in the buffer). This was found not to be the case: in fact, free thiol **3** and Pt complex **1a**·CB[7] exchanges 6 times slower than complexes **3b**·CB[7] and **1a**·CB[7] (conversion rate 7 (± 2) × 10^{-4} s^{-1}; see SI section for a plot of the exchange). To support or invalidate pathway 3, we calculated the stabilities of Pt thiolate **1a**, and of a putative dimer **1a**$_2$ that would lead to ligand exchange, using DFT methods (optimization and vibrational analysis carried out at the b97-3c/def2-mTZVP level in conjunction with the COSMO solvation model; see Figure 7). The calculated free Gibbs energy for the dimerization process is as low as –9.3 kcal/mol (corresponding to a binding constant of 6.0 × 10^6 M^{-1}), and therefore, regardless of the precision of the computational method, significant or predominant dimerization is expected in solution, in strong support for an associative process.

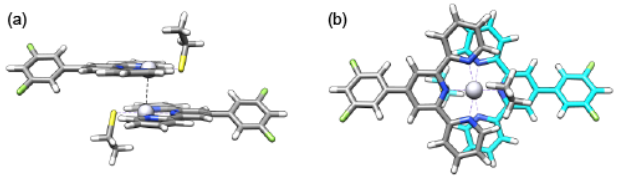

Figure 7. DFT-optimized dimer $\mathbf{1a}_2$ (B97-3c/def2-mTZVP +COSMO); (a) side view, and (b) view along the Pt–Pt axis.

The associative pathway can also rationalize (1) why ligand exchange is dramatically slower in the CB[8]-secured Pt thiolate dimers, and (2) why bulky thiolates such as L-glutathione (**5**) inhibit the exchange. As the pair of CB[8]-bound ternary complexes interact to allow the exchange, the formation of the transition state is severely hindered by the two other Pt complexes sitting on top of the transition state (see Figure 8). The penalty imposed for the distortion of the auxiliary Pt complex to accommodate the neighboring transition state very likely accounts for the severe rate retardation of the ligand exchange process, especially in the case of homoternary complexes bearing two bulky thiolates (see Figure 8a). A slightly less congested assembly can be envisioned when ligand exchange takes place on heteroternary complexes bearing only one bulky thiolate ligand (Figure 8b). These two geometries can be used to rationalize the sigmoidal ligand exchange pattern of the total concentration of Pt complex **1a** when assemblies $\mathbf{1a}_2$·CB[8] and $\mathbf{2b}_2$·CB[8] (or $\mathbf{3b}_2$·CB[8]) are allowed to self-sort (see Figure 6). Ligand exchange is slow while homoternary complexes $\mathbf{1a}_2$·CB[8] and $\mathbf{2b}_2$·CB[8] are the major components of the mixture and adopt the pathway presented in Figure 8a. As the concentration of heteroternary complexes **1a**·**2b**·CB[8] (as well as **1a**·**2a**·CB[8] and **1b**·**2b**·CB[8]) increases due to concomitant supramolecular and slow ligand exchange, the pathway depicted in Figure 8b becomes increasingly prevalent, and further accelerates ligand exchange until equilibrium is reached.

Finally, we do not categorically exclude from consideration the visually appealing intra-assembly exchange of ligands in CB[8]-secured Pt sulfide dimers (see Figure 8c), as rates of ligand exchanges were found to be independent from Pt complex concentration. The geometrical requirements for such a pathway seem too penalizing, however.

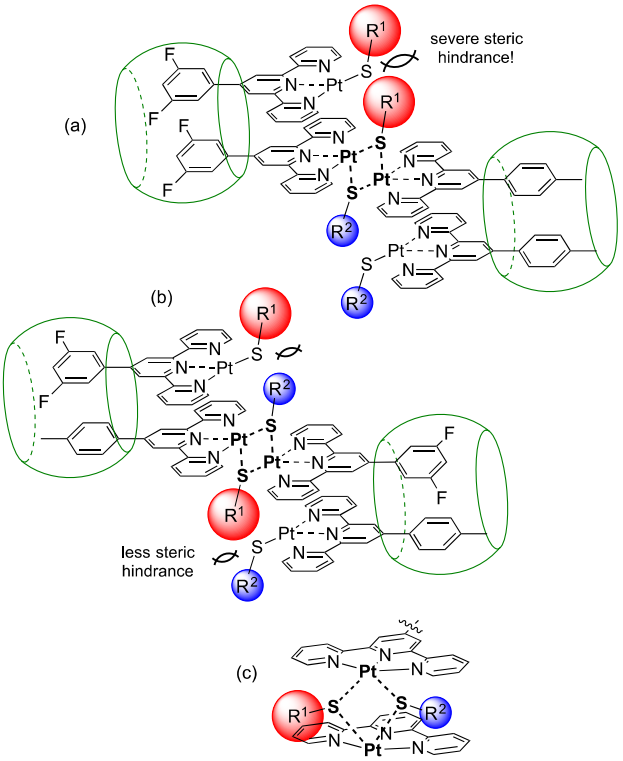

Figure 8. Three possible pathways for ligand exchanges in CB[8]-secured Pt(II) thiolate dimers. Associative pathway between (a) a pair of homoternary complexes, (b) a pair of heteroternary complexes, and (c) two Pt complexes within a CB[8] assembly; 4'-substituents and CB[8] not shown for clarity.

So far, we have shown that rates of ligand exchanges strongly depend on the nature of the thiolate tails, and supramolecular exchanges do not. We also showed that supramolecular exchanges proceed at least 6 times faster than ligand exchanges (in the case of the $\mathbf{1a}_2$·CB[8]/$\mathbf{2b}_2$·CB[8] pair). With the $\mathbf{1a}_2$·CB[8]/$\mathbf{5b}_2$·CB[8] pair, supramolecular exchange proceeds at a rate similar to all other pairs, while ligand exchange is fully inhibited due to the larger size of the L-glutathione tail. What remained to be tested was the impact of the tails on the distribution of the 10 assemblies, a purely thermodynamic matter once equilibrium is reached.

In an earlier study, we developed a scale to characterize the self-sorting process between a pair of guests and CB[8] (see equilibrium 2, for example).[12] Its equilibrium constant K, and corresponding free energy term ΔG, are readily obtained from equation 11. A negative ΔG term indicates social self-sorting (i.e. the preferred formation of heteroternary assemblies), and a positive one indicates narcissistic self-sorting (i.e. the predominance of homoternary assemblies). A ΔG term equal to 0 corresponds to a statistical distribution of homo- and hetero-assemblies (1:1:2), and ΔG terms greater than 2.3 kcal/mol or lower than –2.3 kcal/mol indicate 99% narcissistic or social self-sorting, respectively.[12]

$$\Delta G = -RT \ln K = -RT \ln \frac{\left[\mathbf{1a}\cdot\mathbf{1b}\cdot\mathrm{CB[8]}\right]/2}{\left[\mathbf{1a}_2\cdot\mathrm{CB[8]}\right]^{1/2} \cdot \left[\mathbf{1b}_2\cdot\mathrm{CB[8]}\right]^{1/2}} \quad (11)$$

When complex **1a**$_2$·CB[8] is allowed to scramble with complex **2b**$_2$·CB[8], all 10 resulting assemblies are ultimately at equilibrium with one another. We can thus consider equilibrium 12 to isolate and quantify the impact of the thiolate tails on the distribution of assemblies: the three homo- and heteroternary complexes bear the same difluoroaryl-substituted tpy head (ligand **a**), and the equilibrium thus solely depends on the nature of the thiolate tails.

$$\frac{1}{2}\mathbf{1a}_2\cdot\mathrm{CB[8]} + \frac{1}{2}\mathbf{2a}_2\cdot\mathrm{CB[8]} \rightleftarrows \frac{1}{2}\mathbf{1a}\cdot\mathbf{2a}\cdot\mathrm{CB[8]} + \frac{1}{2}\mathbf{2a}\cdot\mathbf{1a}\cdot\mathrm{CB[8]} \qquad (12)$$

Similar equilibria can be considered when complexes **3a**$_2$·CB[8] to **5a**$_2$·CB[8] are combined with reference assembly **1a**$_2$·CB[8].

Free energy terms equal to –0.05, –0.08 and +0.33 kcal/mol were obtained for the **2a**$_2$·CB[8]/**1a**$_2$·CB[8], **3a**$_2$·CB[8]/**1a**$_2$·CB[8] and **4a**$_2$·CB[8]/**1a**$_2$·CB[8] pairs, respectively. We attribute the barely social behavior of the **2a**$_2$·CB[8]/**1a**$_2$·CB[8] pair (i.e. the slight preference for the formation of heteroternary complex **1a**·**2a**·CB[8]) to possible electrostatic repulsion between the carboxylate units in homoternary complex **2a**$_2$·CB[8]. We use a similar argument to justify the slight preference for the formation of assembly **3a**·**1a**·CB[8], namely the repulsion between the positive ammonium groups in homoternary complex **3a**$_2$·CB[8]. The weak repulsion is very likely caused by the solvation of the charged units that dampens intermolecular interactions. To the contrary, the clearly narcissistic behavior of the **4a**$_2$·CB[8]/**1a**$_2$·CB[8] pair (ΔG = +0.33 kcal/mol) is remarkable, as it suggests a favorable interaction between the cysteine units in homoternary complex **4a**$_2$·CB[8], likely via two carboxylate/ammonium contacts despite heavy solvation of both zwitterions (see Figure 9 for DFT-optimized homo- and heteroternary assemblies).

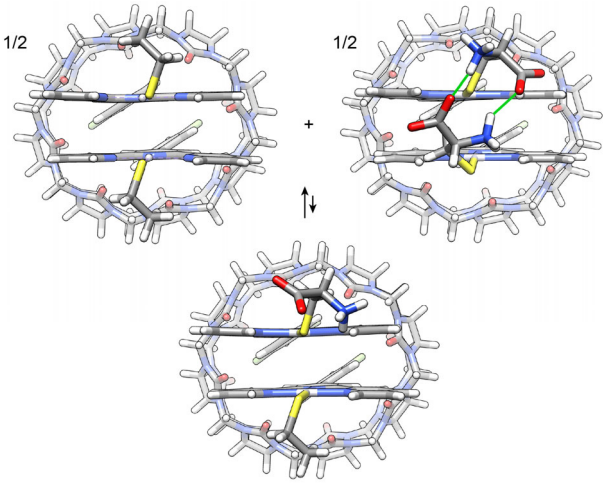

Figure 9. Equilibrium between homoternary assemblies **1a**$_2$·CB[8] and **4a**$_2$·CB[8], and heteroternary assembly **1a**·**4a**·CB[8]. Intra-assembly hydrogen bonds between cysteine units in complex **4a**$_2$·CB[8] are marked in green (DFT optimization at the B97-3c/def2-mTZVP+COSMO level).

CONCLUSIONS

We have shown that a "dual layer" self-sorting system can be designed, in aqueous medium and in situ, from (1) CB[8], (2) a pair of readily synthesized Pt tpy chlorides bearing two different substituents at the 4'-position of the tpy ligand, and (3) two thiols. Up to 10 CB[8]-secured Pt thiolate "stacked" dimers are formed once supramolecular exchanges (understood as the scrambling of the substituted tpy heads inside CB[8]), and thiol ligand exchanges have reached an equilibrium. Supramolecular exchanges are at least 6 times faster than the fastest ligand exchange. Contrary to supramolecular exchanges, the kinetics of ligand exchanges strongly depend on the size of the thiolate tail. For example, no ligand exchange is observed when the thiolate tail is L-glutathione (**5**). CB[8]-secured Pt dimers undergo ligand exchange at least 1,700 times slower than CB[7]-bound Pt monomeric complexes. An associative pathway that involves the formation of dimers of CB[8]-secured Pt dimers (a total of 4 Pt complexes) has been invoked to rationalize these trends.

The thiolate tails also control the distribution of the 10 assemblies at equilibrium. For example, we showed that "intra-assembly" hydrogen bonding between L-cysteine units in assembly **4a**$_2$·CB[8] favors narcissistic self-sorting, i.e. the retention of homoternary complexes to the expense of their heteroternary counterparts. The scope of this result is significant, as these CB[8]-secured Pt dimers can now be used to quantify interactions between virtually any dimer of cysteine-containing peptides. Furthermore, the ease of the in situ preparation of a vast library of functionalized Pt(II) complexes with cysteine-containing peptides could prove useful for the design of cytotoxic agents.[24–29]

ASSOCIATED CONTENT

Supporting Information

Preparation and characterization of Pt(II) complexes/CB[n] assemblies (PtCl·**a**)$_2$·CB[8], (PtCl·**b**)$_2$·CB[8], **1a**$_2$·CB[8], **2a**$_2$·CB[8], **1b**$_2$·CB[8] – **5b**$_2$·CB[8], **1a**·CB[7], **1b**·CB[7], **2a**·CB[7] and **2b**·CB[7]; protocol for kinetic experiments; computational data. The Supporting Information is available free of charge on the ACS Publications website.

AUTHOR INFORMATION

Corresponding Author

* masson@ohio.edu

Notes

The authors declare no competing financial interest.

ACKNOWLEDGMENT

We are grateful to the National Science Foundation (grant CHE-1507321), the American Chemical Society Petroleum Research Fund (grant 56375-ND4), the Roenigk Family Foundation and Ohio University for their continuing financial support. HB is also supported by a fellowship from the Alfonso Martin Escudero Foundation.

REFERENCES

(1) Liu, S.; Ruspic, C.; Mukhopadhyay, P.; Chakrabarti, S.; Zavalij, P. Y.; Isaacs, L. *J. Am. Chem. Soc.* **2005**, *127*, 15959–15967.

(2) Rekharsky, M. V; Mori, T.; Yang, C.; Ko, Y. H.; Selvapalam, N.; Kim, H.; Sobransingh, D.; Kaifer, A. E.; Liu, S.; Isaacs, L.; et al. *Proc. Natl. Acad. Sci.* **2007**, *104*, 20737–20742.

(3) Moghaddam, S.; Yang, C.; Rekharsky, M.; Ko, Y. H.; Kim, K.;

Inoue, Y.; Gilson, M. K. *J. Am. Chem. Soc.* **2011**, *133*, 3570–3581.
(4) Cao, L.; Šekutor, M.; Zavalij, P. Y.; Mlinarić-Majerski, K.; Glaser, R.; Isaacs, L. *Angew. Chemie Int. Ed.* **2014**, *53*, 988–993.
(5) Lee, J. W.; Samal, S.; Selvapalam, N.; Kim, H. J.; Kim, K. *Acc. Chem. Res.* **2003**, *36*, 621–630.
(6) Lagona, J.; Mukhopadhyay, P.; Chakrabarti, S.; Isaacs, L. *Angew. Chemie Int. Ed.* **2005**, *44*, 4844–4870.
(7) Masson, E.; Ling, X.; Joseph, R.; Kyeremeh-Mensah, L.; Lu, X. *RSC Adv.* **2012**, *2*, 1213–1247.
(8) Isaacs, L. *Acc. Chem. Res.* **2014**, *47*, 2052–2062.
(9) Assaf, K. I.; Nau, W. M. *Chem. Soc. Rev.* **2015**, *44*, 394–418.
(10) Murray, J.; Kim, K.; Ogoshi, T.; Yao, W.; Gibb, B. C. *Chem. Soc. Rev.* **2017**, *46*, 2479–2496.
(11) Joseph, R.; Nkrumah, A.; Clark, R. J.; Masson, E. *J. Am. Chem. Soc.* **2014**, *136*, 6602–6607.
(12) Raeisi, M.; Kotturi, K.; Del Valle, I.; Schulz, J.; Dornblut, P.; Masson, E. *J. Am. Chem. Soc.* **2018**, *140*, 3371–3377.
(13) Kotturi, K.; Masson, E. *Chem. - A Eur. J.* **2018**, *24*, 8670–8678.
(14) Tang, B.; Yu, F.; Li, P.; Tong, L.; Duan, X.; Xie, T.; Wang, X. *J. Am. Chem. Soc.* **2009**, *131*, 3016–3023.
(15) Brandenburg, J. G.; Bannwarth, C.; Hansen, A.; Grimme, S. *J. Chem. Phys.* **2018**, *148*, 64104.
(16) Schäfer, A.; Huber, C.; Ahlrichs, R. *J. Chem. Phys.* **1994**, *100*, 5829–5835.
(17) Klamt, A.; Schüürmann, G. *J. Chem. Soc. Perkin Trans. 2* **1993**, No. 5, 799–805.
(18) Castellano, F. N.; Pomestchenko, I. E.; Shikhova, E.; Hua, F.; Muro, M. L.; Rajapakse, N. *Coord. Chem. Rev.* **2006**, *250*, 1819–1828.
(19) Wong, K. M. C.; Yam, V. W. W. *Coord. Chem. Rev.* **2007**, *251*, 2477–2488.
(20) Henderson, R. A. *Kinetics and Mechanism of Reactions of Transition Metal Complexes*; Wiley-VCH Verlag GmbH & Co. KGaA: Weinheim, 2002.
(21) Jordan, R. B. *Reaction Mechanisms of Inorganic and Organometallic Systems*, 3rd ed.; Oxford University Press: Oxford, 2007.
(22) Bugarčić, Ž. D.; Heinemann, F. W.; Van Eldik, R. *J. Chem. Soc. Dalt. Trans.* **2004**, *4*, 279–286.
(23) Petrović, D.; Stojimirović, B.; Petrović, B.; Bugarčić, Z. M.; Bugarčić, Ž. D. *Bioorganic Med. Chem.* **2007**, *15*, 4203–4211.
(24) Rosemberg, B.; Van Camp, L.; Krigas, T. *Nature* **1965**, *205*, 698–699.
(25) Rosenberg, B.; Vancamp, L.; Trosko, J. E.; Mansour, V. H. *Nature* **1969**, *222*, 385–386.
(26) Kelland, L. *Nat. Rev. Cancer* **2007**, *7*, 573–584.
(27) Johnstone, T. C.; Park, G. Y.; Lippard, S. J. *Anticancer Res.* **2014**, *34*, 471–476.
(28) Deo, K. M.; Ang, D. L.; McGhie, B.; Rajamanickam, A.; Dhiman, A.; Khoury, A.; Holland, J.; Bjelosevic, A.; Pages, B.; Gordon, C.; et al. *Coord. Chem. Rev.* **2018**, *375*, 148–163.
(29) Lazarević, T.; Rilak, A.; Bugarčić, Ž. D. *Eur. J. Med. Chem.* **2017**, *142*, 8–31.